ELSEVIER

Journal of Nuclear Materials 271&272 (1999) 405–409

journal of nuclear materials

The use of liquid metals in porous materials for divertor applications

L.I. Ivanov, S.A. Maslyaev, V.N. Pimenov *, E.V. Dyomina, Yu.M. Platov

A.A. Baikov Institute of Metallurgy of Russian Academy of Sciences, Leninsky pr. 49, 117911 Moscow, Russian Federation

Abstract

Features of using capillary porous materials (stainless steel, tungsten, graphite) cooled by liquid lithium for divertor module of thermonuclear fusion reactor have been considered. Temperature distribution in divertor plate under the power density of 10 MW/m^2 was calculated for steady state and pulsed heat influences. The surface temperature as a function of power density and dependence of lithium evaporation yield on temperature was evaluated. Thickness of cover lithium layer with safe porous material against direct pulse heat influence type of plasma disruption (power density in the range of (1–5)10^3 MW/m^2) was estimated. Concerning the problem under consideration, features of hydrodynamic and capillary effects as well as chemical interaction between lithium and investigated materials have been discussed.

1. Introduction

The extension of researches concerning with experimental thermonuclear fusion reactor (TFR) type of TOKAMAK caused the importance of the problem of development of materials which can endure the pulse heat loading above 20 MW/m^2 without plasma contamination of heavy elements. Approximately at the middle of the eighties so called 'sweated' alloys have been included in the list of considered materials. When using these alloys the part of heat loading is sunk due to evaporated components of the material [1–4]. Last time the new structural solution of the high heat sink problem due to evaporation of lithium transported to irradiated surface through capillaries was of some interest [5,6].

In this paper the approach based on the two above mentioned ideas – 'sweating' alloys and capillaries cooled by liquid coolant – have been considered for high heat loaded components of TFR particularly for divertor. The porous materials being the means of transport for liquid coolant (lithium) and structural base have been suggested for the divertor construction. The temperature rise of lithium surface and evaporation yield for different materials, power density and divertor plate thickness have been calculated for divertor module of porous matrix with a liquid lithium cover layer. The three types of heat loading: non-steady state heat influence of beginning stage, steady state heat flux of stable plasma and high heat pulses of short duration (few ms) type of plasma disruption [7,8] have been considered.

2. Non-steady state heat influence on divertor module

The scheme of divertor module manufactured using porous plate (A) of d thickness impregnated by liquid lithium is presented in Fig. 1. On the plasma faced hot surface of temperature T the lithium form the cover layer of thickness d_0. On the back side the plate liquid is streamed by liquid lithium of temperature T_0 circulated in a coolant loop. Heat flux of power density W_0 rises the temperature of free surface of lithium up to maximum T_m. Then steady state is continued up to heat flux to be finished.

The evolution of temperature profile in the porous material during non-steady state heat is determined by solving heat conduction equation taking into account convective heat transfer [9]:

$$\rho' c' (\partial T/\partial t) - Jc(\partial T/\partial x) = \lambda(\partial^2 T/\partial x^2), \quad (1)$$

where ρ' and c' are volume-approximated density and heat capacity of the divertor plate material ($\rho' = \Sigma \rho_i n_i$,

* Corresponding author. Tel.: +7-095 135 9604; fax: +7-095 135 4540; e-mail: pimenov@sci.lpi.msk.su

0022-3115/99/$ – see front matter
PII: S0022-3115(98)00795-8

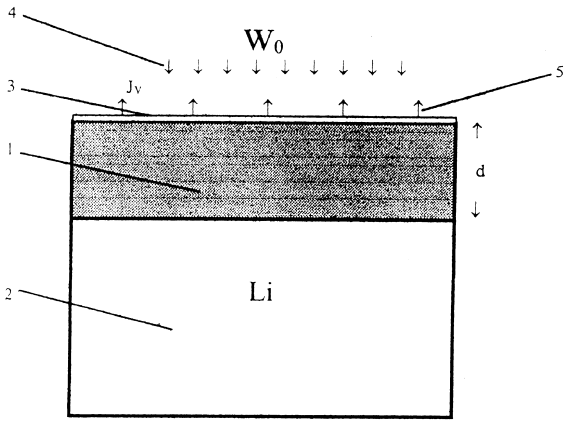

Fig. 1. Model scheme of a porous divertor plate cooled by liquid lithium. (1) Plate, (2) lithium in cooling loop, (3) lithium cover layer, (4) heat flux, (5) evaporating lithium.

$c' = \Sigma c_i n_i$, $i =$ Li, A, n_i is the volume content of lithium and material A), c the specific heat capacity of lithium, J the yield of lithium stream through the porous material ($J = n(\mathrm{Li})\ \rho(\mathrm{Li})v$, where v is velocity of the stream), λ is the effective thermal conductivity of divertor plate ($\lambda = \Sigma \lambda_i n_i$, $i =$ Li, A), x-direction of heat flux, $x = 0$ and $x = d$ correspond to free surface of lithium and the back side surface of the plate respectively (see Fig. 1). It was assumed that surface porosity is equal to volume one and capillary channels are interconnected.

The numerical calculation of the temperature $T(x,t)$ was carried out for following initial and boundary conditions:

$$T(x,0) = T_0,$$
$$T(d,t) = T_0, \qquad (2)$$
$$(\partial T/\partial x)_{x=0} = -(W_0 - W_V)/\lambda,$$

where W_V is the part of power density for lithium evaporation. To determine $J = J(T)$ in Eq. (1) it was assumed that the yield of lithium stream through the porous plate is equal to the yield of lithium evaporation $J_V = J$, and the value $J_V = J_V(T)$ was calculated using the formula [10]

$$J_V = \alpha P(T)(2\pi RT/\mu)^{-1/2}, \qquad (3)$$

where α is the coefficient of evaporation (for assumed condition $\alpha \sim 1$ Ref. [10]), $P(T)$ is the vapour pressure, R is the gas constant, μ is the atomic mass of lithium.

The temperature distribution in the plate for stainless steel–20 vol.% Li and W–20% Li has been calculated for thickness $d = 1$ mm and $d = 4$ mm under power density $W_0 = 10$ MW/m^2. In Fig. 2 the temperature distribution in the plate for W–20% Li for thickness $d = 1$ mm under power density $W_0 = 10$ MW/m^2 are presented as an example. In both cases the temperature in the plate of 4 mm thickness becomes steady not later than 4 s after heating begins. For the 1 mm thickness plate this time was of one order smaller. For both materials the steady state distribution of temperature is linear. The maximum temperature T_m of lithium surface for porous tungsten plate was 150° for $d = 1$ mm and 250° for $d = 4$ mm lower than for porous steel plate. This fact results from the higher thermal conductivity of tungsten. Corresponding estimations for a divertor module of porous graphite (graphite–20 vol% Li) show results similar to those in Fig. 2 with numerical data being between values corresponding to W–20% Li and steel–20% Li.

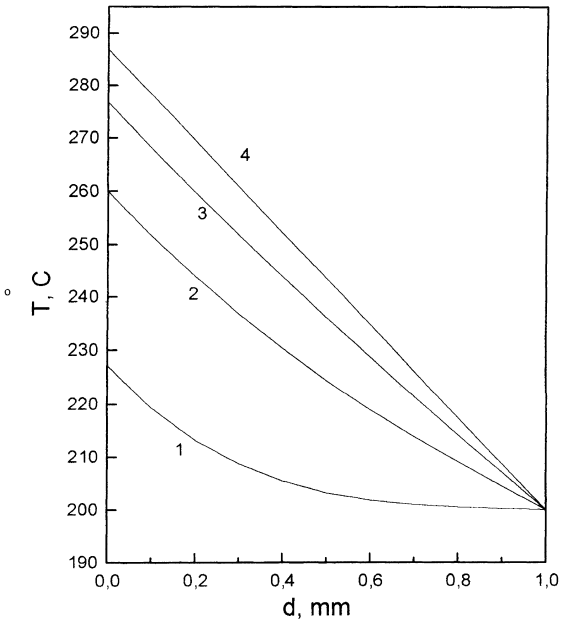

Fig. 2. Temperature distribution in divertor plate for W-20 vol% Li ($d = 1$ mm) compositions for different time under power density $W = 10$ MW/m^2. (1) $t = 0.01$ s, (2) $t = 0.05$ s, (3) $t = 0.1$ s, (4) $t = 0.2$ s.

So calculations have demonstrated rapid stabilisation of thermal state under considered heat conditions for selected materials.

3. Steady state heat influence

The balance equation for steady conditions may be presented as follows:

$$W_0 = W_C + W_T + W_V, \qquad (4)$$

where W_C is the power density spent to heating lithium when it streams through the divertor plate from the cold ($T = T_0$) to the hot ($T = T_m$) one, W_T power density sunk

due to heat conduction, W_V is the power density for lithium evaporation. In steady state when the temperature distribution is linear (see Fig. 2) the addenda in the right-hand side of Eq. (4) may be presented as follows:

$$W_C = cJ(T)(T_m - T_0), \tag{5}$$

$$W_T = \lambda(T_m - T_0)/d, \tag{6}$$

$$W_V = HJ_V(T), \tag{7}$$

where H is the heat of evaporation of lithium and as assumed above $J_V(T) = J(T)$.

Substituting Eqs. (3), (5)–(7) to balance Eq. (4) we can solve it and determine the temperature on the surface of the divertor plate T_m as a function of incident power density. Corresponding numerical calculations have been carried out for three types of porous materials impregnated by liquid lithium: tungsten, stainless steel and graphite. Calculation results for three different thickness of W–20 vol.% Li divertor plate are presented in Fig. 3. When the surface temperature is below 600°C the curve $T_m(W_0)$ is linear. When the surface temperature is higher than 600°C the curve is found to deviate from the straight line: because of Lithium evaporation the temperature rise decreases with the increasing of W_0. This fact is noticeable for steel whose heat conductivity is lowest [11]. So as heat conductivity of tungsten is highest the surface temperature of tungsten plate was significantly smaller than ones of steel and graphite under the same power density.

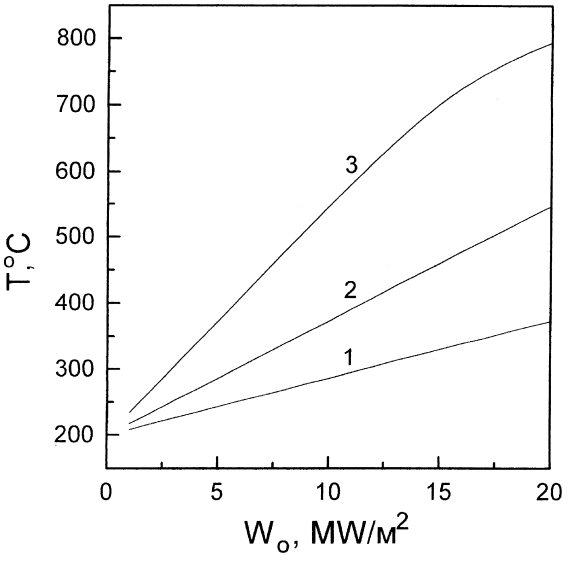

Fig. 3. The surface temperature of divertor plate as a function of power density for W–20 vol.% Li plates of different thickness. (1) $d = 1$ mm, (2) $d = 2$ mm, (3) $d = 4$ mm.

To estimate the velocity of the lithium stream through the porous material the calculation of evaporation yield as a function of temperature was carried out using the formula Eq. (3). The estimations show that at $T = 600$°C evaporation yield is of ~2.3 g/s per square metre. This value increases approximately by one order of magnitude with a 100°C increasing of temperature. The velocity of the lithium stream through 20% porous material at 600°C to compensate the loss is given by $V = J_V/\rho(\mathrm{Li})n(\mathrm{Li})$ ~23.5 μm/s and shows a sharp increase with temperature increasing.

The numerical estimation based on Eq. (1) for porous tungsten and graphite plates of 1 and 4 mm thickness shows that increasing lithium velocity even up to a few mm/s will not influence the temperature distribution in the plate. Significant decrease in surface temperature are found at velocities above $V = 0.01$ m/s. Realisation of such velocity of coolant stream through porous capillary channels seems to be impossible.

4. Pulse heat influence type of plasma disruption

Under power pulse heat influence type of plasma disruption simulated (power density W_P ~10^3 MW/m^2 and pulse duration τ~few ms) materials not only melt but efficiently evaporated [12,13]. In the model we considered the incident heat flux deposited in both the cover lithium cover layer and underlying porous material impregnated by lithium. The cover layer would be a safeguard enough if all pulse power would be deposited in the layer and be spent for heating and evaporation of lithium. In this case the underlying porous material would not be influenced by undesirable excess heating.

Assuming that all incident heat power during the pulse duration τ is spent in heating and evaporation of lithium the thickness Z may be estimated:

$$Z = W_P\tau/\rho(c\Delta T + H), \tag{8}$$

where ΔT is the difference between boiling temperature of lithium $T_V = 1336$°C and surface temperature before heat pulse influence. The value $Z = Z(W_P)$ was calculated particularly for $\tau = 5$ ms and $\Delta T = 800$°C. The average values of c and ρ in this range of temperature were used. Z linearly increases from 400 μm to 0.22 cm under power density is varied from 10^3 to 5×10^3 MW/m^2. In other words to save the porous material against pulse heat influence with power density of $W_P = 5 \times 10^3$ MW/m^2 and time $\tau = 5$ ms, the lithium cover layer thickness should fit the condition $d \leqslant 0.22$ cm.

It should be noted that this estimation does not take into account heat conduction into the bulk because of the small pulse duration. More exact estimations would gives lower value of critical thickness Z.

5. Discussion

5.1. Interaction of liquid coolant with divertor material

Liquid coolant penetrating through the capillary of porous material step increase self temperature from $T = T_0$ to $T = T_m$ with intensity of corrosion processes increasing: dissolving of solid matrix, grain boundary penetration, forming of intermetallic compounds on interphase boundary. From this point of view, liquid lithium is highly aggressive with reference to structural stainless steels of different sorts under temperature in the range of 500–600°C [14–18]. However corrosion resistance of steels could be increased due to variation of alloy composition [17,18].

In thick ($d = 4$ mm) steel divertor plates under heat power density of 10 MW/m^2 the plasma faced temperature rises to ~800°C. Under this temperature the corrosion of steel in lithium and evaporation yield of lithium are highly intensive. Using more thin plates ($d = 1$ mm and $d = 2$ mm) the temperature can be decreased down to 450°C and 650°C under the same power density. In this case the corrosion would be sharp suppressed and porous stainless steel cooled by liquid lithium may be considered as promising material for divertor.

Features of interaction between graphite and liquid lithium are mainly concerned with two factors: dissolution of carbon in liquid and possibility of forming of intermetallide Li_2C_2 [19]. As a rule the dissolving (diffusion of carbon to liquid phase) is dominant in comparison with reactive growth of solid intermetallide [20]. Using graphite of 50% porosity the temperature of the divertor surface under power density of 10 MW/m^2 rises to 500°C for $d = 2$ mm and to 350°C for $d = 1$ mm. Under those temperatures the saturated contents of carbon in lithium are of 1.3 and 1.0 at.% and at lithium melt temperature it is of about 0.5 at.%. The possibility of dissolving of carbon in lithium melt make some difficulties of using the porous graphite as a structural material. The lithium alloyed by carbon or other component may be used as a coolant to reduce the dissolving. Determination of optimal composition of the coolant needs special investigation.

Concerning chemical interaction between carbon and lithium it should be taken into consideration that the rate of diffusion growth of stoichiometric intermetallic compound Li_2C_2 at low temperatures ($T < 400$°C) is negligible.

It should be noted that graphite, unlike steel and tungsten, has significant advantage: under high power pulses due to plasma disruption it is sublimated but not melted and will not reduce the penetrativeness of the capillary porosity. This fact permits us to reduce the thickness of lithium cover layer and to avoid undesirable hydrodynamics effects.

Amongst considered porous materials the tungsten is most corrosion resistant under liquid lithium environment. The solubility of tungsten in lithium in temperature range of 650–1150°C is 1.7×10^{-11}–4.3×10^{-6} at.% [21]. The solubility of lithium in tungsten is also negligible [22].

Temperature calculations show that a plasma facing surface of porous tungsten plate of $d = 4$ mm under power density of 10 MW/m^2 is heated up to $T_m = 550$°C. For thinner plates ($d = 2$ and 1 mm) surface temperature is of 375°C and 280°C, respectively. These values are highly lower than corresponding temperatures for porous graphite and steel.

5.2. Hydrodynamic and hydrostatic effects

In thermonuclear devices the surface of divertor may be inclined at different angles to the gravitation vector g_0 (see for example the scheme of ITER [23]), so liquid phase under gravity force may change initial shape and run down. In this case the cover lithium layer could be held on the divertor surface by capillary forces of surface tension only. Gravity force could result in deformation of the free surface of the liquid phase, non-uniformity of liquid layer thickness, formation of droplets and falling down of droplets.

Noted effects could reduce the safeguard part of the lithium layer and promote damage of divertor module especially under plasma disruption when surface could be melted [12,13] and penetrativeness of capillary porosity could be reduced. So the effects need special research out of the frames of present work. The preliminary analysis shows that in low gravity conditions being characterised by low gravity vector $g = \beta g_0$, where $\beta < 10^{-3}$ [24], considered effects would be negligible due to dominant part of capillary forces on the liquid surface. The conclusion is made that use of porous materials with a liquid cover layer in energy systems at the space apparatus (orbital stations, sputniks and so on) are promising. In this case the coolant expense and capillary porosity penetrativeness limitations would be reduced due to sharp decreasing effect of flow down of liquid.

6. Conclusions

1. The features of capillary porous materials cooled by liquid coolant being used for divertor modules have been considered.
2. Using a model scheme of a divertor plate based on porous stainless steel and tungsten of 20 vol.% porosity as well as graphite of 20 and 50 vol.% porosity the calculations of temperature distribution have been carried out for different values of plate thickness un-

der steady state and non-steady state heat influences of varied heat power density.

3. When there are no differences between evaporation and penetration yields of lithium, it have been found that under the heat power density of 10 MW/m^2 the plasma facing surface of divertor plate of 2 mm thickness was heated up to 400°C for W–20% Li, 600°C for graphite–20% Li and 700°C for steel–20% Li.
4. The evaporation yield of lithium as a function of temperature was calculated. At 600°C the lithium cover layer loses approximately 2.3 g/s per square meter and a velocity of lithium penetration through 20% porous divertor plate should be of about 24 μm/s to compensate the loss.
5. The thickness of lithium layer which could protect the divertor surface under direct influence of high heat pulse types of plasma disruption have been estimated. Under power densities in the range of (1–5)10^3 MW/m^2 and pulse duration of 5 ms, the thickness of lithium layer being heated and evaporated was of the (400–2200) μm.
6. The features of chemical interaction between liquid coolant and porous material have been discussed in terms of dissolution and phase transformation processes. On the base of this analysis and numerical calculations results the porous tungsten, graphite and austenitic stainless steel cooled by liquid lithium could be considered as promising materials for the divertor module of the thermonuclear fusion reactor.
7. It has been noted that in low gravity conditions in space apparatus the positive role of capillary forces for the formation of the surface shape of a cover layer of liquid coolant would be increased significantly, with the coolant expense and capillary porosity penetrativeness limitations being reduced due to sharp decreasing of liquid flow down effect.

Acknowledgement

This work was supported by INCO-COPERNICUS (Grant No. ERB IC15 CT98 0911).

References

[1] G.G. Bondarenko, L.I. Ivanov, S.I. Kucheryavyi, Phys. Chem. Mater. Treatment 3 (1985) 53.
[2] B. Baretzky, W. Eckstein, R.P. Schorn, J. Nucl. Mater. 224 (1995) 50.
[3] L.I. Ivanov, V.L. Markushev, S.A. Maslyaev, V.N. Pimenov, M.E. Reznitsky, I.P. Sasinovskaya, A.B. Tsepelev, Phys. Chem. Mater. Treatment 2 (1995) 24.
[4] L.I. Ivanov, A.P. Komissarov, V.A. Polyakov, Phys. Chem. Mater. Treatment 3 (1995) 18.
[5] L.G. Golubchikov, V.A. Evtikhin, I.E. Lyublinsky, V.I. Pistunovich et al., Seventh International Conference on Fusion Reactor Materials, Obninsk, 25–29 September 1995, p. 76 (Abstracts).
[6] V.I. Pistunovich, A.V. Vertkov, V.A. Evtikhin, V.M. Korjavin et al., Seventh International Conference on Fusion Reactor Materials, Obninsk, 25–29 September 1995, p. 70 (Abstracts).
[7] I.V. Altovsky, S.P. Grachev, L.I. Ivanov, Yu.M. Platov, Phys. Chem. Mater. Treatment 2 (1986) 9.
[8] S.A. Maslyaev, Yu.M. Platov, V.N. Pimenov, Phys. Chem. Mater. Treatment 4 (1990) 9.
[9] A.V. Lykov, Heat and Mass Transfer, Handbook, Moscow, Energia, 1978, 479 p.
[10] A.N. Nesmeyanov, Vapour Pressure of Chemical Elements M. Publ. AS USSR, 1961, 396 p.
[11] A.P. Babichev et al., Physical Values. Handbook, in: I.S. Grigoryev, E.Z.M. Melihov (Eds.), Energoatomizdat, 1991, 1232 p.
[12] S.A. Maslyaev, V.I. Neverov, V.N. Pimenov, Yu.M. Platov, C. Ya Betsofen, I.P. Sasinovskaya, Phys. Chem. Mater. Treatment 2 (1993) 42.
[13] L.I. Ivanov, S.A. Maslyaev, V.L. Markushev, V.N. Pimenov et al., J. Adv. Mater. 2 (4) (1995) 290.
[14] D.F. Teortorelli, H. De Van, J. Nucl. Mater. 141–143 (1986) 579.
[15] G.M. Gryaznov, V.A. Evtihin, L.P. Zavyalsky et al., Atom. Energia. 59 (5) (1985) 355.
[16] G.M. Gryaznov, L.G. Golubchikov, V.A. Evtihin et al., Atom. Energia 59 (5) (1985) 358.
[17] I.E. Lublinsky, E.V. Dyomina, V.A. Evtihin, M.D. Prusakova et al., Phys. Chem. Mater. Treatment 3 (1990) 131.
[18] A.V. Vertkov, V.A. Evtikhin, I.E. Lyublinski, E.V. Demina et al., J. Nucl. Mater. 203 (1993) 158.
[19] T.B. Massalski (Ed.), Binary Alloy Phase Diagrams, American Society for Metals, Metals Park, OH 44073, vol. 1, 1986, p. 571.
[20] K.P. Gurov, B.A. Kartashkin, Yu.E. Ugaste, Heterodiffusion in Polyphase Metal Systems, Nauka, GRFML, 1981, 350 p.
[21] J. Sungster, A.D. Pelton, J. Phase Equilibria 12 (2) (1991) 203.
[22] P.A. De Mastry, Nucl. Appl. 3 (2) (1967) 127.
[23] W.B. Gauster, J. Nucl. Mater. 212–215 (1994) 3.
[24] L.I. Ivanov, V.S. Zemskov, L.I. Kubasov, V.N. Pimenov et al., Melting, Crystallisation and Phase Formation Under Weightlessness Conditions, Nauka, 1979, 255 p.